STUDIES ON THE MECHANICAL PROPERTIES AND MICROSTRUCTURE OF PULSED TIG WELDED JOINTS OF Al-Mg-Si ALLOYS

A DISSERTATION

Submitted in partial fulfillment of the
requirements for the award of the degree
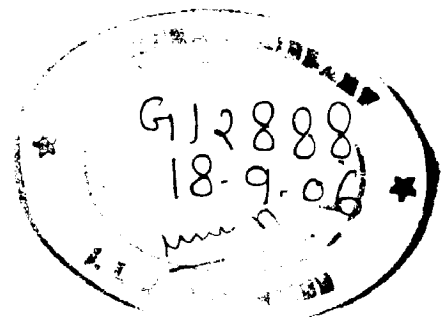*of*
MASTER OF TECHNOLOGY
in
MECHANICAL ENGINEERING
(With Specialization in Welding Engineering)

By

JAYA RAJESH MANTI

DEPARTMENT OF MECHANICAL AND INDUSTRIAL ENGINEERING
INDIAN INSTITUTE OF TECHNOLOGY ROORKEE
ROORKEE-247 667 (INDIA)
JUNE, 2006

CANDIDATE'S DECLARATION

I hereby declare that the work which is being presented in the dissertation entitled "STUDIES ON THE MECHANICAL PROPERTIES AND MICROSTRUCTURE OF PULSED TIG WELDED JOINTS OF Al-Mg-Si ALLOYS", in partial fulfillment of the requirement for the award of the degree of **Master of Technology** in **Mechanical Engineering** with specialization in **Welding Engineering**, submitted in the Department of Mechanical and Industrial Engineering, Indian Institute of Technology Roorkee, Roorkee, is an authentic record of my work carried out over a period of eight months from NOVEMBER 2005 to JUNE 2006, under the supervision of **Dr.D.K.Dwivedi**, Assistant Professor, Department of Mechanical and Industrial Engineering, Indian Institute of Technology, Roorkee and **Mr. Ajay Agarwal**, Assistant Professor, Department of Mechanical and Industrial Engineering, Indian Institute of Technology, Roorkee.

The matter embodied in this dissertation has not been submitted for the award of any degree.

Dated: June 30, 2006   (JAYA RAJESH MANTI)

Place: Roorkee   M.Tech. II Year

                                              Dept. of Mech. & Ind. Engg.

CERTIFICATE

This is to certify that the above statement made by the candidate is correct to the best of my knowledge.

(Mr. AJAI AGARWAL)   (Dr. D.K.DWIVEDI)

Asst. Prof,   Asst. Prof,

Dept of Mech. & Ind. Engg.,   Dept of Mech. & Ind. Engg.,

I.I.T.Roorkee,   I.I.T.Roorkee,

Roorkee- 247667.   Roorkee- 247667.

Acknowledgement

I wish to express my deep sense of gratitude and sincere thanks to my loving guides **Mr. AJAI AGARWAL and Dr. D.K.Dwivedi,** Department of Mechanical and Industrial Engineering, IIT Roorkee, for being helpful and a great source of inspiration. Their keen interest and constant encouragement gave me the confidence to complete my work. I wish to extend my sincere thanks for their excellent guidance and suggestions for the successful completion of my seminar work.

I offer my sincere thanks to all staff of welding research laboratory, I.I.T., Roorkee for their help and cooperation throughout the course of this work.

I am also thankful to all my friends for their continuous support and help during different stages of my project work

(JAYA RAJESH MANTI)

ABSTRACT

Pulsed TIG in its simplest form is a system in which the arc current alternates between two levels, heating and fusion take place during the periods of higher current, with cooling and solidification during the periods of low current. PGTAW process optimizes the heat input with proper heat distribution while maintaining stable arc characteristics.

The heat-treatable 6000 series Al Mg Si alloys, with medium to high strength, excellent formability and good corrosion resistance, possess great application potential in industries. These alloys are principally used in automotive, pipe, structural, railings and extruded parts.

In this work, Al-Mg-Si alloys were welded by Pulsed TIG welding process to investigate the influence of pulse frequency, peak current, pulse duration and duty cycle on microstructure and mechanical properties such as hardness and tensile strength.

It was observed that pulse TIG welding produced finer grain structure of weld metal than conventional TIG welding. Hardness was found higher for shorter pulse duration. High tensile strength was also observed with shorter duty cycles than longer duty cycles.

CONTENTS

LIST OF TABLES

LIST OF FIGURES

INTRODUCTION

Presently Tungsten Inert Gas (TIG) welding process is one of the most well established processes which can not only weld all metals of industrial use but also gives the best quality welds amongst the arc welding processes [1].A non consumable tungsten electrode is used in this process with an inert gas shield.

In pulsed TIG process, the current is supplied in pulses rather than at constant magnitude. The aim of pulsing is mainly to achieve maximum penetration without excessive heat build-up, by using the high current pulses to penetrate deeply and then allowing the weld pool to dissipate some of the heat during a proportionately longer arc period at a lower current. Earlier studies on pulse TIG process emerged reports of reduced distortion, improved bead contour, reduced susceptibility to hot tearing and reduced grain size. The increased number of variables in the pulsed TIG welding process also supports the possibility of increased control of solidification [2].

Properties such as high strength to weight ratio, good corrosion resistance and ease of fabrication apart from high electrical and thermal conductivity make aluminium alloys versatile and attractive for many engineering applications. Al-Mg-Si alloys (6XXX series) are the most frequently used heat-treatable aluminium alloys. These alloys are commonly used as auto-body parts, parts machined from plate or bar, piping, among many others. Fabrication of these alloys frequently needs welding for joining the structural elements [3]

Literature did not reveal detailed studies on the influence of pulse parameters of TIG welding on microstructure and mechanical properties of Al-Mg-Si alloys. This work has been carried out to study the influence of pulse parameters such as pulse duration, pulse frequency, duty cycle and peak current on microstructure and mechanical properties of Al-Mg-Si weld joints produced by TIG welding.

LITERATURE REVIEW

2.1 TIG Welding Process

The tungsten inert gas (TIG) welding uses a non consumable tungsten electrode for one terminal of the arc which is with an inert gas. The electrode is used only to create an arc. The arc fuses the metal being welded as well as the filler if it is used. The gas shield protects the electrode, weld pool and surrounding HAZ, and provides the required arc characteristics. The process may employ either DCEN or AC. In general balanced AC is preferred for welding aluminum and magnesium and their alloys and some grades of stainless steels.

TIG provides the optimum weld quality and a superior penetration bead, while accommodating a wider range of thicknesses, positions, and geometries than either SMAW or MIG. Today TIG is one of the most well established processes which can not only weld all metals of industrial use but also gives the best quality welds amongst the arc welding processes

The TIG process has advantages over the other welding processes which in many cases make it more desirable to use. Some of these advantages are:

    i. Highly Concentrated Arc.

    ii. Inert Gas Shielding:

    iii. No Flux or Slag:

    iv. No Smoke or Fumes:

    v. No Sparks or Spatter:

2.2 TIG welding power source

With TIG welding, the operator has three choices of welding current. They are: direct current electrode negative (straight polarity), direct current electrode positive (reverse polarity), and alternating current with high-voltage high-frequency arc stabilization. Each of these current types has its applications and its advantages and disadvantages.

2.2.1 Direct Current Electrode Negative (DCEN or Straight Polarity)

In Direct current electrode negative (DCEN), the torch is connected to the negative terminal of the power source and work lead is connected to the positive terminal. When the arc is established, electron flow is from the negative electrode to the positive work piece. In a DC arc approximately 70% of the heat will be concentrated at the positive side of the arc, therefore the greatest amount of heat is distributed into the work piece. This accounts for the deep penetration obtained when using DCEN for GTAW welding. The electron flow leaving the electrode results in a cooling effect on the tungsten; therefore it operates at a lower temperature

2.2.2 Direct Current Electrode Positive (DCEP or Reverse Polarity)

When Direct Current Electrode Positive (DCEP) is used the torch is connected to the positive terminal, and the ground or work lead is connected to the negative terminal. When using this polarity, the electrode receives the greatest amount of heat and becomes very hot. The electrode must be large even when low amperages are used to prevent overheating and possibly melting the electrode. The work piece receives a smaller amount of the total heat resulting in shallow penetration. The positive gas ions are now attracted to the negative work piece. They strike the work with sufficient energy to chip away the brittle aluminum oxides and provide "cleaning action." Cleaning action refers to the breaking up and removal of the oxide coating. Because of this beneficial oxide removal, this polarity would seem to be excellent for welding aluminum and magnesium.

2.2.3 Alternating Current

A compromise to obtain the advantages of both DCEN and DCEP is to use alternating current. During a complete cycle of alternating current there is theoretically one half cycle of electrode negative and one half cycle of electrode positive. In theory, the half cycles of alternating current are of equal time and magnitude. Tests show that the half cycles are unbalanced, the electrode positive half cycle being of lesser magnitude

3

2.3 Pulsed TIG

Pulsed TIG in its simplest form is a system in which the arc current alternates between two levels, heating and fusion take place during the periods of higher current, with cooling and solidification during the periods of low current. Continuous fusion along a seam is achieved by ensuring that the individual weld spots overlap. The relationship between the current pulses and the fused spots is shown in Fig.2.1.

Welding current pulsation techniques have recently been introduced, and increased weld reproducibility and quality have been reported as a consequence. This 'pulsed arc' technique as it is known is particularly significant in welding thin gauge materials. Periodic interruption of the welding current permits interpulse cooling, which reduces the heat spread in advance of the weld pool and consequently reduces the degree of distortion produced during welding.

Basically pulsed arc equipment is that of standard TIG with slight electrical modification to provide for current pulsing. The modulated welding current produced consists usually of a low power pilot arc upon which are super-imposed higher current pulses. The superimposed high current pulse is generally of a square wave form and of sufficient magnitude and duration to form a weld pool. The pilot arc does not contribute to melting directly, as it is present only to maintain the arc during the periods of low current, after the high current pulses. The significance of pulsed current for tungsten arcs has yet to be evaluated in terms of melting efficiency, metallurgical properties of the weld, and operational characteristics [4].

R.G.Dickens observed that for maximum penetration, pulse amplitude was more beneficial than pulse duration. Pulsed TIG weld dimensions of penetration, width and fused area were all greater than for continuous TIG, when based on an equivalent average current. Pulsed TIG welds gave less distortion than continuous TIG welds. Pulsed TIG is particularly suited to the welding of sheet less than 1cm thick as it reduces the risk of burn through.

In short, PGTAW process optimizes the heat input with proper heat distribution while maintaining stable arc characteristics. PGTAW process offers many advantages in welding thin sections such as pipe, tube, parts for heat exchangers, chemical vessels and various other components used in the field of nuclear and aerospace industry. Important

welding parameters in PGTAW process are high current level, low current level, high current duration, low current duration and pulsing frequency apart from other usual parameters like welding speed, arc gap etc. Weld made with pulsing parameters generates less weld stress compared to steady current welding confirming better heat utilization..

High current level (Peak pulse current) is of primary importance since it predicts the weld heat input. Increased current produces higher weld pool temperature resulting in more fluidity and hence the spreading of the weld bead occurs. The low current level is also called as back ground current. The value of background current decides the heat input to the work piece if the pulse current is constant. This current affects the rate of cooling and solidification [5].

The duration of high current level should be long enough to negate the effects of the variable stepping phenomena, but short enough to minimize the heat input. Back ground duration is selected empirically to be long enough to avoid heat build-up and usually works out to be not less than the pulse duration and not more than three times the pulse duration.

Pulse duty cycle can be defined as the fraction of time period of the pulse. Higher pulse duty cycle indicates the tendency towards continuous current. The increase in pulse duty cycle causes increase in heat input resulting deeper penetration and wider weld bead.

When the pulse frequency is increased the pulse time reduces. This shall reduce the radiation loss per pulse. The total radiation losses per second shall be the product of heat loss per pulse multiplied by number of pulses. The total radiation and convective losses increase with increasing frequency. This results in reduced penetration and weld width and increased width of HAZ.

Welding voltage affects the penetration and weld width. Increase in welding voltage reduces the penetration and increases the weld width because at higher welding voltage arc becomes wider and heat per unit area decreases. Welding speed is another dominating factor in defining the geometry of the bead. With increase in welding speed the heat per unit length decreases and hence both weld width and penetration are reduced. When gas flow rates are very high, the spattering takes place and irregular shape is obtained. Though with increase in gas flow rate the penetration and weld width are found to increase first then reduce due to increasing heat losses by radiation and convection.

The pulsed GTA welding process has many specific advantages compared to conventional GTA welding such as:

1. Reduction of the heat input required.

2. Increased weld bead depth to width ratio.

3. Narrower heat affected zone.

4. Reduction of grain size.

5. Reduced tendency to hot cracking.

6. Increased arc stability.

2.4 Shielding Gas

The importance of atmospheric shielding is reflected in the fact that all arc welding processes take their names from the method used to provide the shielding; Gas Tungsten Arc, Gas Metal Arc, Submerged Arc, Shielded Metal Arc, Flux Cored, etc. Primarily two inert gases are used for shielding purposes for TIG. They are argon and helium. Shielding gases must be of high purity for welding applications. The purity required is at a level of 99.995%. The characteristics and a comparison of these gases are as follows:

2.4.1 Argon

When choosing a shielding gas, a fact that must be considered is the ionization potential of the gas. Ionization potential is measured in volts and is the point where the welding arc will be established between the electrode and the work piece through the shielding gas. In other words, it is the voltage necessary to electrically charge the gas so that it will conduct electricity. The ionization potential of argon is 15.7 volts. So this is the minimum voltage that must be maintained in the welding circuit to establish the arc or to weld with argon. Argon has low thermal conductivity which means it is not a good conductor of heat. This results in a more compact, higher density arc. Arc density refers to the concentration of energy in the arc. With argon this energy is confined to a narrow or more "pinpointed" area. Argon provides excellent arc stability and cleaning action even at low amperages.

2.4.2 Helium

Due to the higher thermal conductivity of helium, the arc column expands, reducing current density in the arc. The arc column will become wider and more flared out than the arc column with argon shielding gas. The more flared out the arc column, the more work surface area is being heated. The heat at the center of the arc can move more readily downward toward the colder metal at the bottom of the work piece. This results in a deeper penetrating arc.

Helium is not as desirable as argon for manual welding applications. Because of its higher ionization potential, it is more difficult to start an arc with helium shielding gas, especially at lower amperages. Because helium is a light gas, flow rates are usually two or three times higher than argon for equivalent shielding. The cost of helium is considerably more than argon, and with the increased flow rate, total cost of shielding goes up sharply.

2.5 Electrodes

TIG electrodes are the final link in the chain between the power source and the weld. They are classified as non consumable. Electrodes for TIG welding arc almost entirely made from tungsten which has melting temperature of 3370 C and boils at 6135 C[7]. Tungsten electrodes are classified on the basis of their chemical compositions, as summarize in Table 2.1, taken from ANSI, AWS A5.12-92.

In the AWS classification system, E stands for an electrode, which is used as one terminal of the arc welding circuit. The W stands for the chemical symbol for tungsten (also called wolfram). The final letter indicates the alloying element or oxide addition. P designates a pure tungsten electrode without intentional alloying elements, while all other designations are for certain oxides additions. Zr is for zirconiated, Th for thoriated, Ce is ceriated, La is lanthanated and G stands for unspecified oxide additions. Finally the numbers specify the nominal alloying composition (in weight percent). For example, EWTh-1 is a thoriated tungsten electrode that contains nominally 1% thoria.

2.5.1 Pure Tungsten Electrodes (EWP):

Pure tungsten electrodes (EWP) contain a minimum of 99.5 wt-% tungsten, with no intentional alloying elements, as summarized in table 2.1. The current carrying capacity of pure tungsten electrode is lower that that of the alloyed tungsten electrodes. Pure tungsten electrodes are least expensive and used mainly with alternating current (AC) for welding of aluminum and magnesium alloys, because DC welding with pure tungsten electrode typically produces small amounts of tungsten inclusions (discontinuities) in welds.

2.5.2 Zirconiated Tungsten Electrodes (EWZr-1):

Zirconiated tungsten electrodes (EWZr-1) contain a small amount (0.15 to 0.40 wt-%) of zirconium oxide (ZrO_2). Zirconiated tungsten electrodes have welding characteristics that generally fall between those of pure tungsten and thoriated tungsten electrodes. They are normally the electrodes of choice for AC welding of aluminum and magnesium alloys because they combine the desirable arc stability characteristics of pure tungsten along with higher current carrying capacity and better arc starting characteristics of thoriated tungsten electrode

2.5.3 Thoriated Tungsten Electrodes (EWTh-1 and EWTh-2):

Thoriated oxide (ThO_2), which is called thoria, is another oxide used to alloy tungsten electrodes. Two types of thoriated tungsten electrodes are readily available (Table 2.1). The EWTh-1 electrodes contain a nominal 1 wt% thoria and the EWTh-2 electrodes contain a nominal 2 wt% thoria, evenly dispersed throughout their entire lengths. Thoriated tungsten electrodes are superior to pure tungsten electrodes in several respects. The thoria is responsible for increasing the usable life of these electrodes and also reduces the electrode tip temperatures and provides greater resistance to contamination of the weld.

The EWTh-1 and EWTh-2 tungsten electrodes were designed for direct current electrode negative (DCEN) or straight polarity application and are desirable for the welding of steels, nickel alloys, and most alloys other than aluminum and magnesium.

2.5.4 Ceriated Tungsten Electrodes (EWCE-2):

The EWCe-2 electrodes are tungsten alloy electrodes that contain a nominal 2 wt% cerium oxide (CeO_2, referred to as ceria). These electrodes were developed as a possible

replacement for thoriated tungsten electrodes because ceria, unlike thoria, is not a radioactive material. They tend to have longer life than thoriated tungsten electrodes. EWCe-2 electrodes can operate successfully with AC and DC.

2.5.5 nthanated Tungsten Electrodes (EWLa-1):

The lanthanated tungsten electrodes (EWLa-1) were developed as the ceriated tungsten electrodes for the same reason; that is lanthanum is not radioactive. These electrodes contain a nominal 1 wt% lanthanum oxide (La_2O_2, referred to as lanthana). The current carrying levels, advantages and operating characteristics of these electrodes are very similar to the ceriated tungsten electrodes.

2.5.6 Other Tungsten Alloy Electrodes (EWG):

The EWG electrode classification was assigned for alloys not included in the above classes. These electrodes contain an unspecified addition of some oxide or combination of oxides (rare earth or others). The purpose of the addition is to improve the nature or characteristics of the arc, or the life of the electrode (Table 2.1).

2.6 Electrode Size and Current Carrying Capacity:

Tungsten electrodes are available in a variety of standard diameters (sizes) from 0.30 to 8.00 mm. Length from 6mm to 150 mm is typically used. The choices of an electrode classification, size and welding current are influenced by the type and thickness of base metals being welded. The current carrying capacities of all types of tungsten electrodes are affected by the type of welding torch, the type of power source, the electrode extension beyond the collet, and the shielding gas.

In an arc, approximately 70% of heat is generated at the anode and 30% heat at the cathode. When the electrode is negative, it can carry a much higher current without overheating than when the electrode positive. Direct current with the electrode positive requires a much larger diameter to support a given level of current because the tip is not cooled by the emission of electrons but is heated by their impact. In general, an electrode of a given diameter operating on DC electrode positive(DCEP or reverse polarity) would be expected to handle only 10% of the current possible as compared with the electrode being negative (DCEN or straight polarity). Therefore, much larger electrodes are required for DCEP [6].

With balanced alternating current, the tip is cooled during the electrode negative half cycle and heated when positive. Therefore, the current carrying capacity of an electrode operating on AC is between that of DCEN and DCEP. In general, it is about 50% less than that of DCEN. Operating at current levels exceeding those recommended of a given electrode size and tip configuration may cause the tungsten to erode, melt or split. Tungsten particles may fall in into the weld pool and become discontinuities or defects in the weld. Operating at current levels too low for a specific electrode diameter can result in arc instability. Use of the smallest recommended diameter for the current level is usually best.

2.7 Al-Mg-Si Alloy

The demand for more lightweight, fuel efficient and enhanced performance automobiles stimulates the research and development of high-strength and high formability aluminium alloys. The heat-treatable 6000 series Al Mg Si alloys, with medium to high strength, excellent formability and good corrosion resistance, possess great application potential in the automobile industry and have been subjected to extensive research [7].

The solidification behaviour of binary Al-Mg alloys is relatively simple. While in the Al-Mg-Si alloys with less than 2 wt% Mg and less than 1 wt% Si, the as-cast microstructure is fairly complicated. It means that the addition of silicon has great influence on the solidification path of the alloys. Kang.S.B. and Liu.Y.L, observed that the magnesium content in the alloys greatly influenced the as-cast microstructure. The higher the magnesium content, the more Mg2Si structure was present. In the high magnesium alloys, not only binary eutectic structure, but also ternary eutectic structure formed [8].

Necessary condition for liquation cracking in Al-Mg-Si welds: For liquation cracking to occur in full-penetration welds, there must be a higher fraction solid (or more precisely, a higher strength) in the weld metal than in the PMZ during PMZ terminal solidification [9].

Both the ductility and the tensile strength show little or no correlation with the bulk porosity content, especially in the case of samples containing dross and oxide films.

In contrast, the mechanical performance decreases monotonically with an increase in the area fraction of defects in the fracture surface of the samples. The projected area fraction of defects in a given cross section of the sample seems to determine the effect of casting defects on the tensile behaviour[10].

The tensile fracture of cast Al–Si–Mg alloys with structural defects can be explained in terms of the principles of fracture mechanics. The presence of structural defects in a cast Al–Si–Mg alloy will have the general effect of reducing elongation in a tensile test. Tensile specimens without structural defects are likely to achieve high values for elongation, and fracture will most probably initiate from clusters of fractured silicon particles[11].

The failure of Al–Si–Mg alloys is generally accepted to occur in three stages: (1) silicon particle cracking at low plastic strains; (2) as deformation proceeds, cracked particles generate localized shear bands which form microcracks by joining adjacent cracked particles; and (3) microcracks coalescence followed by propagation, leading to final fracture [12].

EXPERIMENTAION

3.1 Base Material

In present investigation, two compositions of Al-Mg-Si alloys have been used as a base metal. Chemical compositions of the base material have been shown in Table 3.1. Specimens having dimensions 90 X 60 X 7 mm were used for investigation were prepared via foundry routine.

3.2 Proportioning of the Charge

To calculate the charge, the chemical composition of all its components and of the alloy to be produced must be known. In addition the melting loss must be taken into account, and this depends on the design and type of melting unit, melting techniques, the method of refining, etc. Assume the following charge components: Primary aluminum ingot and hardeners-- Al-10%Mg, Al-17%Si, Charge is calculated for both alloy compositions [Table 3.2]

3.3 Filler Material

The 6xxx alloys should not be welded with base alloy filler or without a filler addition, because it can result in cracking. These are most easily welded with the aluminium-silicon type filler alloys. In this investigation, 1.6mm diameter Al-5%Si (A-404) filler material has been used.

3.4 Preparation of weld joint

Welding was carried out on CEBORA 360, which is a semi automatic machine. The following few parameters were kept constant during the investigation:

1. Electrode material was 2% thoriated tungsten Electrode.

2. Electrode size was 3.5 mm diameter.

3. Shielding gas was a mixture of 98%Argon and 2% Oxygen.

4. Arc length was maintained at 2.5 mm.

5. Arc travel speed was maintained at 6.1 cm/min.

6. Arc voltage was maintained at 19 volts.

7. Shielding gas flow rate was maintained at 12 L/min.

The 7 mm thick Al-Mg-Si plate of 90 X 60 square mm was mechanically cleaned by grinding and wire brushing. One long edge of the plate machined to have 30° groove angle and 1.5 mm root face. Hence, total groove angle was 60°. Schematic diagram of joint is shown in Fig.3.1. The grooved faces of two plates were firmly tack welded at both the ends maintaining a root gap equal to 1mm.The plates were firmly held in position by using a fixture automatic system was used to move the torch at desired speed for welding in single pass. The diameter of filler wire, composition of shielding gas mixture and its flow rate as well as contact tip to work piece distance were maintained constant throughout the experiment.

The pulsed TIG welding has been carried out with two set of parameters. In first set, 160A and 180A peak currents, 0, 25, 50 and 100 pulse frequencies, 4ms and6ms pulse durations are used. In second set welding was done at a peak current of 250A, a background current of 125A with 25, 33 and 50Hz pulse frequencies at 40% and 50% duty cycles. During welding at any pulse parameters, the arc voltage was kept constant at 19 ± 0.5 V by suitable adjustment in power source. During welding, the welding speed has been kept constant at 6.1 cm/min. After welding the weldments were cutted for the preparation of samples to investigate the microstructure, harndness and tensile strength Fig.3.2.

3.5 Metallurgical characteristics

3.5.1 Specimen preparation

For metallographic examination the specimen were collected from the middle portion of the weldments to ensure a true representation of weld characteristics. The specimens were cut into suitable size and transverse section of the welds were polished by using various grades of emery papers (200, 500, 800, 1000 grade.) from coarse to fine in sequence. Finally the specimens were polished on a polishing wheel, having velvet cloth mounted on it, revolving at a speed of about 600 r.p.m.. Specimens were etched with mixture of dilute HF. The microstructure of the specimens was studied under optical microscope (MM6, Leitz).

3.6 Mechanical testing

The mechanical properties of the weldments were studied by testing hardness, both micro and normal hardnesses, tensile strength of the weld metal. The specimens

were collected from the stable weld region by discarding the run-on and run-off portion of the weld. The specimens for tensile strength were prepared after machining the top and root enforcement of the weld. Tensile tests also have been conducted on specimens, which were heat treated for 30 minutes at 500°C, followed by water quenching and artificial ageing at 200°C for 2 hours. The specimens were machined to size conforming the relevant ASTM and DIN standards.

3.6.1 Hardness testing

Vicker's hardness measurement was carried out by diamond indentation on the metallographically polished and etched transverse section of the weld joint along the central line, at a load 5N. The diagonal length of the indentation were measured and the mean of the two diagonals was used to find out the hardness from the standard chart. Three hardness indentations were set at the center of weld, at fusion zone and at the middle of these two. Micro hardness measurement was carried out (Leitz, microhardness tester) at a load of 100gm. The indentations were set at an interval of 2mm along the weld centre, transverse to the direction of weld deposition.

3.6.2 Tensile Testing

The tensile test specimen of both the weldment and base material were machined out conforming to DIN 50215 standard Fig.3.3 [10]. The tensile testing was carried out on a hydraulically operated tensile testing machine, having a maximum load capacity of 60 KN under static load condition. The load was uniaxially applied on the specimen at a cross head speed of 1mm/min. The ultimate tensile strength was determined by dividing the maximum load by original cross sectional area of the specimen.

3.7. Heat treatment

Tensile test specimens were heat treated to investigate the influence of heat treatment on microstructure and mechanical properties of weldments and base alloys. Heat treatment consist of solutionization at 500^0C for 30 minutes followed by water quenching at room temperature, artificial ageing at 190^0C for 120 minutes and natural ageing for 96 hours.

RESULTS AND DISCUSSION

4.1 First set of parameters

In the first set of parameters, specimens of alloys A and B used for investigation were welded by using 160A and 180A peak currents, 25, 50 and 100Hz pulse frequencies and 4ms and 6ms pulse durations.

4.1.1 Microstructure

In case of microstructure, the influence of peak current and pulse frequency are found to be most important. In general, significant variation in microstructure from base metal to weld center line was observed. As we move from base metal towards weld center line initially coarsening of grains was noticed. Results showed that pulse parameters such as pulse frequency, pulse duration and peak current affect the grain structure of weld metal. Aluminium grains in weld metal are finer than those of base metal, HAZ and fusion boundary.

Micro structures of base metal of alloy A and alloy B are shown in Fig. 4.1(a) and 4.1(b) respectively. Base metals showed mainly two phases i.e., aluminium solid solution grains (α-aluminium, light etched) and low melting temperature eutectic along the grain boundary (dark etched). Fraction of eutectic was found less in alloy B than alloy A.

4.1.1.1 Influence of pulse frequency

Grain structure of HAZ and weldment produced by conventional TIG welding was found coarser than that of pulse TIG welding. The influence of the pulse frequency on microstructure is shown in Fig. 4.3 and 4.4. Increasing the pulse frequency from 25 Hz to 50 Hz coarsens the microstructure of weld deposit to a great extent. But with a further increase in pulse frequency to 100Hz the weld deposit regained the fine dendritic microstructure. Aluminium solid solution (α- Aluminium) was found more in HAZ and fraction of eutectic found more in weld zone, because filler metal Al-5%Si produced more amount of eutectic.

4.1.1.2 Influence of peak current

The influence of the peak current microstructure is shown in Fig. 4.2. Fusion zone showed very fine equiaxed grain structure consisting grains of aluminium solid solution and eutectic (Al-Si) mixture along the grain boundary(Fig. 4.2 b, d). Grain structure of HAZ produced by pulse TIG welding is coarser than that produced by without pulsing (continuous welding).

4.1.1.3 Influence of pulse duration

The influence of pulse duration on microstructure is shown in Fig. 4.5. It was observed that for a given pulse frequency short pulse duration (4 ms) produces finer grain than that for longer pulse duration (6 ms). Aluminium grains produced using 6ms pulse duration were found to be coarser than conventional TIG welding (without pulsing) irrespective of pulse frequency.

4.1.2. Hardness

Influence of pulse frequency, pulse duration and peak current on microhardness and normal (macro) hardness of alloys A and B under study is shown in Tables 4.1 and 4.2. Results showed that the effect of pulse frequency on microhardness is determined by pulse duration and peak current.

Microhardness vs distance from fusion boundary relationship at different welding current is shown in Fig. it can be observed that microhardness is low at fusion boundary compared to that of HAZ near to fusion zone. In general, higher welding current produces greater microhardness at fusion boundary and in HAZ as well [Fig4.8]

4.1.2.1 Influence of pulse frequency

Microhardness (HV_{100}) of weld metal of alloy A produced by using 160A and 180A peak currents and 4ms pulse duration showed that increase in pulse frequency from 0 to 25 Hz decreases the microhardness followed by continuous increase in the hardness up to 100Hz pulse frequency. At 6ms pulse duration, microhardness decreased from 0 to 25Hz pulse frequency followed by increase up to 50Hz only. Pulse frequency corresponding to peak hardness of weld metal was found a function of both pulse duration and peak current [Table 4.1].

Microhardness (HV_{100}) of weld metal of alloy B produced by using 160A and 180A peak currents and 4ms pulse duration showed that increase in pulse frequency from 25 to 100 Hz increases the microhardness continuously. At 6ms pulse duration, this increase in microhardness was found up to 50 Hz followed by decrease at 100 Hz.

Pulse frequency corresponding to least hardness of weld metal was found a function of both pulse duration and peak current. Least hardness was noticed at 6ms and 100Hz for both 160A and 180A peak currents [Table 4.1].

Microhardness vs. distance from fusion boundary relationship for weld joint produced of HAZ using different pulse duration at 25, 50 and 100Hz is shown in Fig. it can be seen that microhardness at fusion boundary of weld joint produced using 4ms is higher than that produced using 6ms irrespective of pulse frequency. Peak microhardness value and distance of peak hardness region from the fusion boundary appear to be a function of pulse duration [Fig.4.9]

4.1.2.2 Influence of pulse duration

Macrohardness (5 Kg) of weld metal of alloy A produced by using 160A and 180A peak currents and 6ms pulse duration showed a continuous decrease in the hardness from 0 to 100Hz pulse frequency. For 4ms pulse duration also same result was found except an increase in macro hardness at 100 Hz for 4ms and 180A peak current. Peak hardness of weld metal was found with continuous welding for both peak currents [Table 4.3].

Macrohardness (5 Kg) of weld metal of alloy B produced by using 180A peak current and 4ms and 6ms pulse durations showed a continuous increase from 25 to 100 Hz pulse frequency. At 160A peak current and 6ms pulse duration macro hardness was found decreasing with the increase in pulse frequency from 25 to 100Hz. At 4ms and 160A peak current, an increase in macro hardness from 25 to 50Hz followed by a reduction from 50Hz to 100Hz was noticed [Table 4.3].

Microhardness vs. distance from fusion boundary of HAZ of weld joints produced using different pulse frequencies is shown in Fig. High microhardness of the fusion boundary was observed at high pulse frequency compared to that low frequency. Lowest

fusion boundary hardness was observed at 25Hz pulse frequency. Peak microhardness value and distance of peak hardness region from the fusion boundary appear to be a function of pulse frequency [Fig 4.10].

4.2 Second set of parameters

In the first set of parameters, specimens of alloys A and B used for investigation were welded by using 125A back ground current, 250A peak current, 25, 33 and 50Hz pulse frequencies and 40% and 50% duty cycles.

4.2.1. Microstructure

In case of second set of parameters also significant variation in microstructure from base metal to weld center line was observed. As we move from base metal towards weld center line initially coarsening of grains was noticed. Aluminium grains in weld metal are finer than those of base metal, HAZ and fusion boundary.

4.2.1.1 Influence of pulse frequency

The influence of the pulse frequency on microstructure is shown in Fig. 4.6. Increasing the pulse frequency from 25 Hz to 33 Hz coarsens the microstructure of weld deposit to a great extent. But with a further increase in pulse frequency to 50Hz the weld deposit regained the fine dendritic microstructure. Aluminium solid solution (α-Aluminium) was found more in HAZ and fraction of eutectic found more in weld zone, because filler metal Al-5%Si produced more amount of eutectic.

4.2.1.2 Influence of duty cycle

The influence of the duty cycle microstructure is shown in Fig. 4.7. It was found that for a given pulse frequency short duty cycle (40%) produces finer grain than that for longer duty cycles (50%). Aluminium grains produced using pulse current were found to be coarser than conventional TIG welding (without pulsing) irrespective of pulse frequency and pulse duty cycle.

4.2.2. Hardness

Influence of pulse frequency, duty cycle and peak current on microhardness and normal (macro) hardness of alloys A and B under study is shown in Tables 4.3 and 4.4.

18

Results showed that the effect of pulse frequency on microhardness is determined by duty cycle and peak current.

4.2.2.1 Influence of pulse frequency

Microhardness (HV_{100}) of weld metal of alloy A produced by using 125A back ground current, 250A peak current and 40 duty cycle showed that increase in pulse frequency from 25 to 50 Hz decreases the microhardness continuously. At 50% duty cycle, microhardness decreased from 25to 33Hz pulse frequency followed by increase at 50Hz [Table 4.2].

Microhardness (HV_{100}) of weld metal of alloy B produced by using 125A back ground current, 250A peak current and 40% duty cycle showed that increase in pulse frequency from 25 to 33Hz increases the microhardness and further increase in pulse frequency causes decrement in microhardness. At 50% duty cycle, this decrease in microhardness was found up to 33Hz followed by increase at 50 Hz. [Table 4.2].

Macrohardness (5 Kg) of weld metal of alloy A produced by using125A back ground current, 250A peak current and 40 duty cycle showed a continuous increase in the hardness from 25 to 50Hz pulse frequency. For 4ms pulse duration a continuous decrease in the hardness from 25 to 50Hz pulse frequency was recorded [Table 4.4].

Macrohardness (5 Kg) of weld metal of alloy B produced by using 125A back ground current, 250A peak current and 40%and 50% duty cycles showed a continuous decrease from 25 to 50 Hz pulse frequency [Table 4.4].

4.2.3. Tensile strength

Tensile tests were performed on specimens of alloy A and alloy B produced by using 125A background current and 250A peak current, at two different duty cycles i.e., 40% and 50% and at three pulse frequencies i.e., 25Hz, 33Hz and 50Hz, to evaluate the ultimate tensile strength (UTS). Four samples for each set of parameters were tested and average values are given in Table 4.5.

For alloy A, ultimate tensile strength was found decreasing for increase in pulse frequency from25Hz to 50Hz at both 40% and 50% duty cycles. For alloy B, UTS was decreasing from 25 to 33Hz followed by increase at 50Hz with both duty cycles [Table 4.5]. Ultimate tensile strength was higher in the case of alloy B for all cases except at

25Hz and 40% duty cycle. For alloy A at 40% duty cycle, UTS recorded for 25 and 33Hz pulse frequency was higher than that of 50% duty cycle. For alloy B at 50% duty cycle, higher UTS was recorded at 33 and 50Hz pulse frequencies than that of 40% duty cycle.

4.2.4. Scanning Electron Microscope (SEM)

To investigate the mode of failure, SEM micrographs of tensile test specimens were taken at 200 X magnification [Figure 4.11]. SEM micrographs showed the failure in the case of alloy B was largely brittle (cleavage type). It shows that failure is of brittle kind. In alloy A micrographs, more dimples are visible, suggesting the ductile failure. For alloy B, dimples are more because of ductile mode of failure.

4.2.3 Heat treatment

One sample for each condition in second set of parameters was heat treated to investigate the influence of heat treatment on microstructure and tensile strength. The influence of heat treatment on microstructure of alloys A and B is shown in Fig. 4.12. Microstructures of alloy A and alloy B without any heat treatment are shown in Fig.4.12 (a, b).when these micrographs are compared with heat treated (i.e., solutionization at 500^0C for 30 minutes followed by water quenching at room temperature, artificial ageing at 190^0C for 120min and natural ageing for 96 hours) refinement of grains was noticed in heat treated specimen's micrographs. Artificial ageing alone is also giving good appearance of grains than the micrographs of samples which have not received any heat treatment.

The influence of solutionization and artificial ageing on hardness of alloys A and B is shown in Table.4.6. For alloy A maximum hardness was recorded with the samples with both solutionization and artificial ageing, and minimum hardness was recorded with the samples of no heat treatment. For alloy B also the maximum hardness was found with heat treated samples.
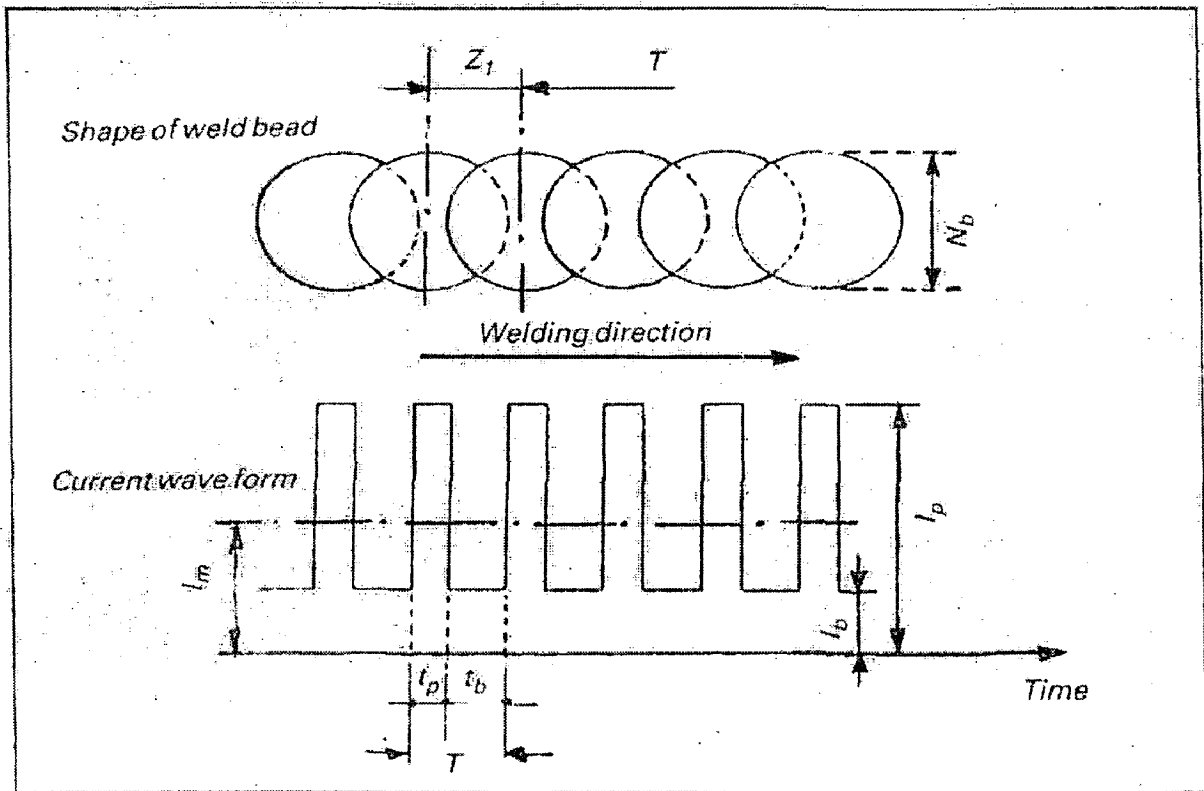
Figure 2.1: The relationship between the current pulses and the fused spots.

Sl. No.	AWS Classification	Colour	Alloying Element	Alloying Oxide
1	EWP	Green	-	-
2	EWCe-2	Orange	Cerium	CeO_2
3	EWLa-1	Black	Lathanum	La_2O_3
4	EWTh-1	Yellow	Thorium	ThO_2
5	EWTh-2	Red	Thorium	ThO_2
6	EWZr-1	Brown	Zirconium	ZrO_2
7	EWG	Gray	Not Specified	-

Table 2.1: Colour Code and Alloying Elements for various Tungsten Electrode Alloys.

Alloy	Magnesium	Silicon	Aluminium
A	0.8	0.6	Balance
B	0.5	0.5	Balance

Table3.1: Composition of Al-Mg-Si alloy used in present investigation.

	Al	Mg	Si	Total
Total required composition for alloy A (in Kg)	98.586	0.824	0.606	101.016
Total required composition for alloy B (in Kg)	99.99	0.515	0.505	101.01

Table 3.2: Charge calculation for Alloys A and B
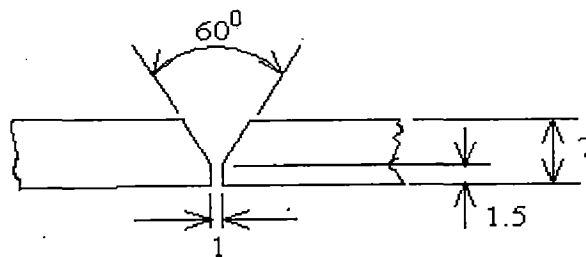
Figure 3.1: Schematic diagram of welding joint

To be discarded   Tensile specimens   To be discarded

Metallographic specimen
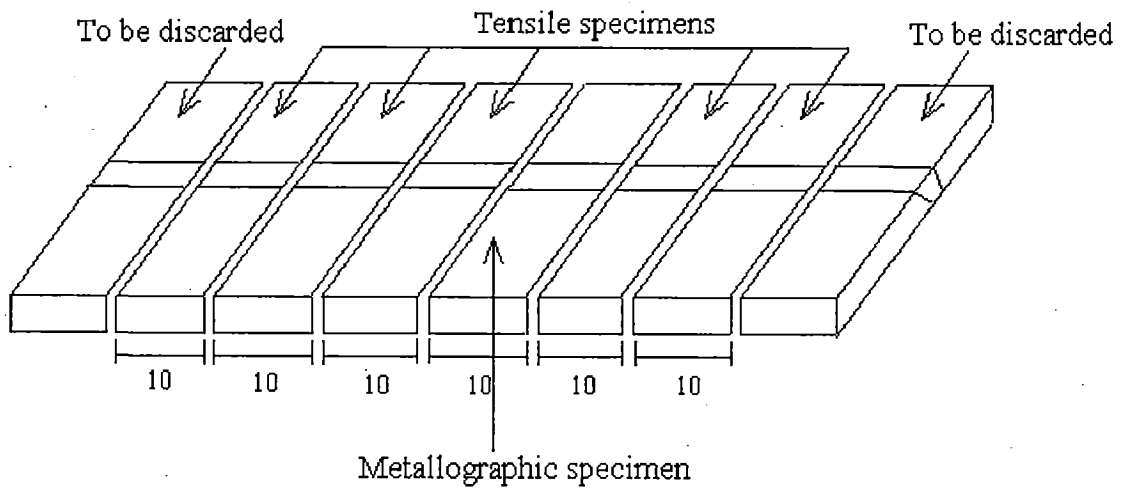
Figure 3.2: Schematic diagram showing how specimens were cut.
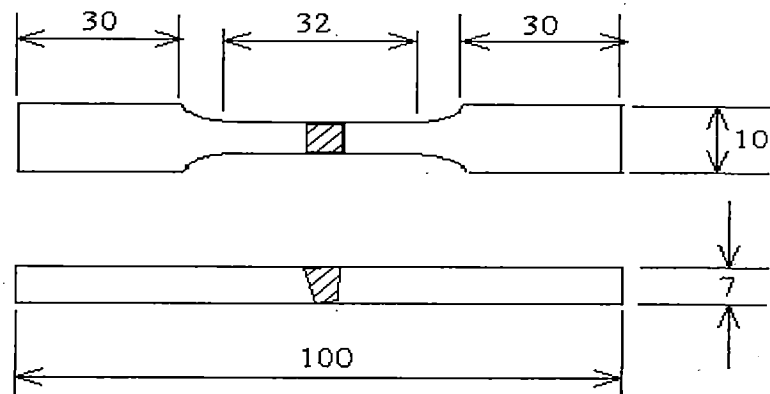
Figure 3.3: Schematic diagram of tensile test specimen.
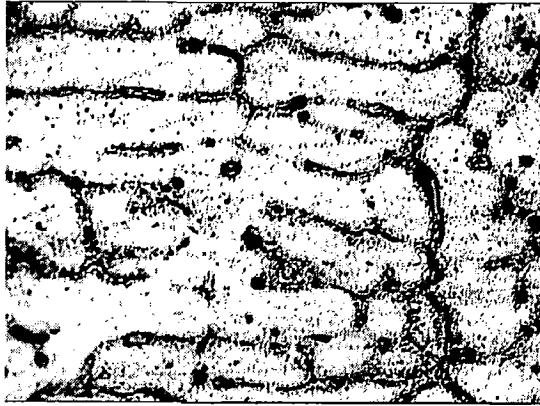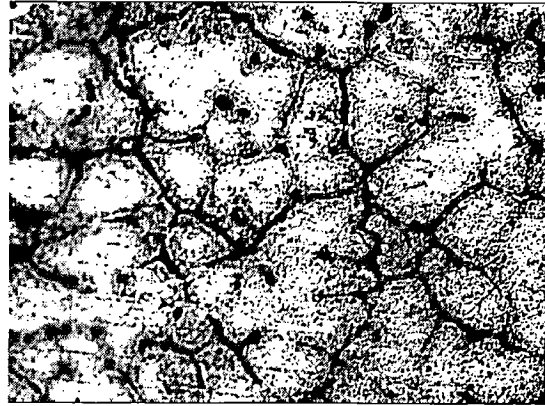
(a)   (b)

Figure 4.1: Optical microstructure of base metals of (a) Alloy A and (b)Alloy B, 200x.
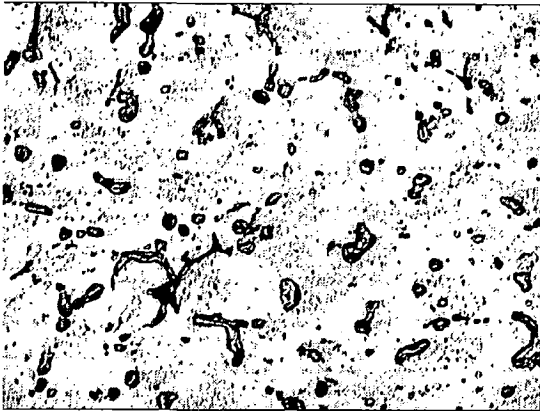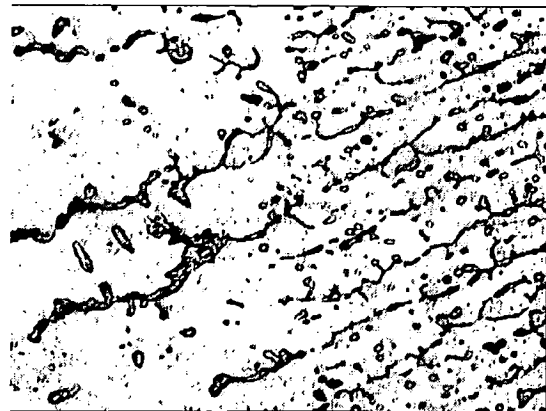
(a) HAZ, 160 Amp   (b) Fusion Boundary, 160 Amp
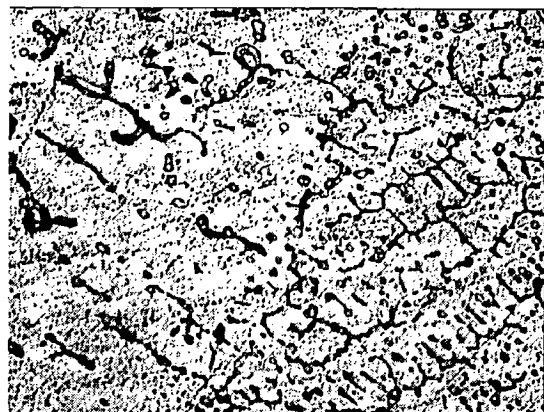
(c) HAZ, 180 Amp   (d) Fusion Boundary, 180 Amp

Figure 4.2: Optical micrograph of HAZ (a, c) and fusion boundary (b, d) of Alloy A weld joints produced using 160 A and 180 A welding current, 200 x.
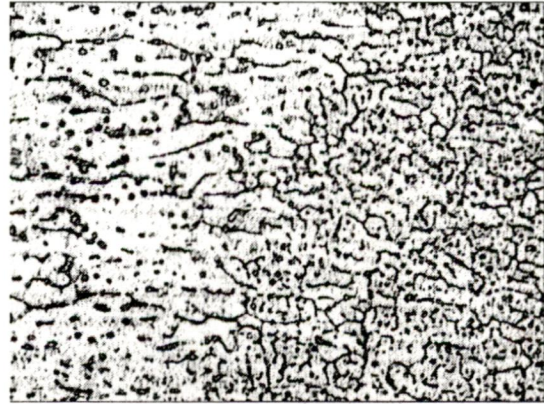
24

(a) HAZ, 25Hz

(b) Fusion Boundary, 25 Hz
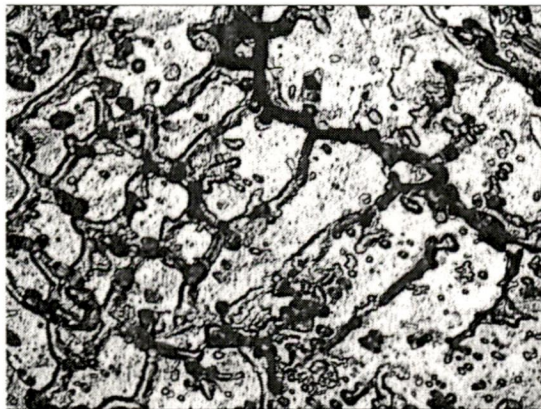
(c) HAZ, 50Hz
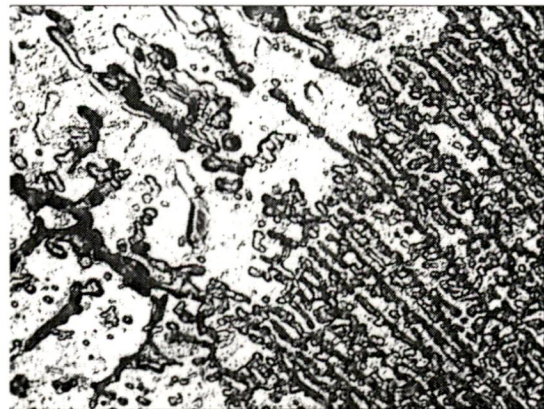
(d) Fusion Boundary, 50 Hz

(e) HAZ, 100Hz
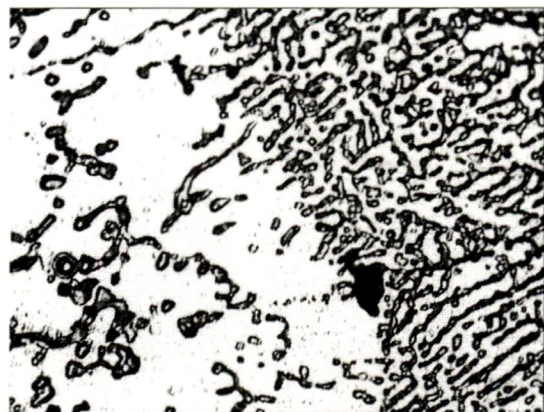
(f) Fusion Boundary, 100 Hz

Figure 4.3: Optical micrograph of HAZ (a, c, e) and fusion boundary (b, d, f) of Alloy A weld joints produced using 25Hz, 50Hz and 100 Hz pulse frequency and 4ms pulse duration, 200x.
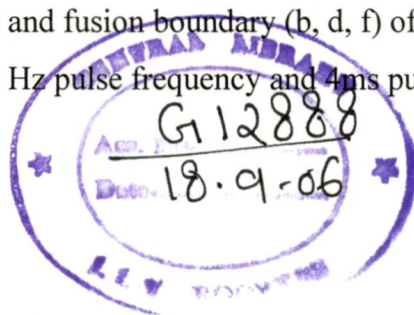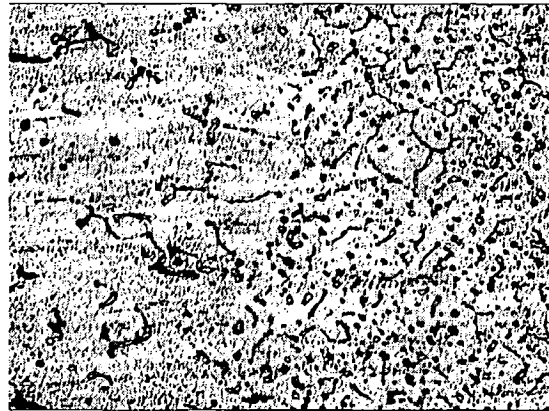
(a) HAZ, 25Hz (b) Fusion Boundary, 25 Hz
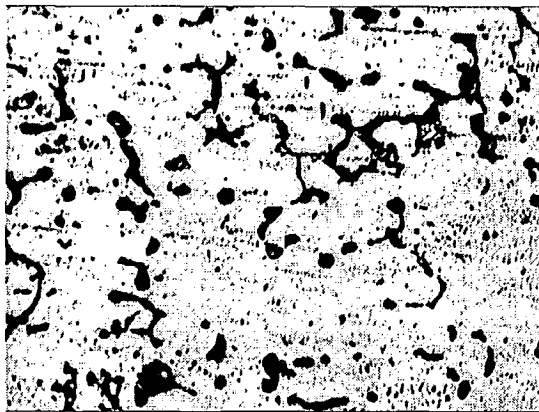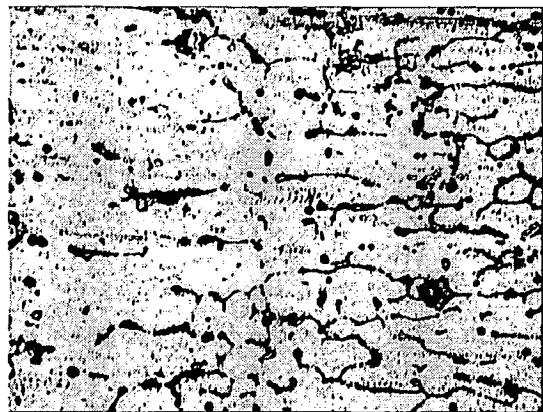
(c) HAZ, 50Hz (d) Fusion Boundary, 50 Hz
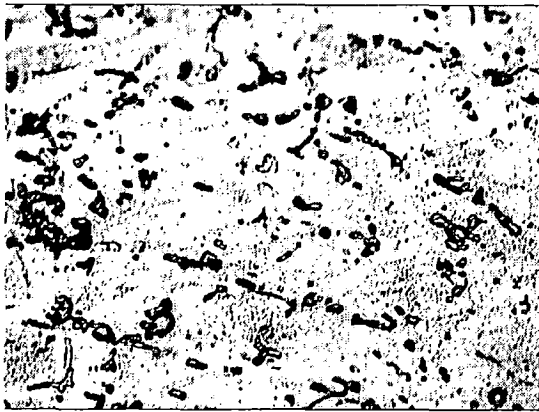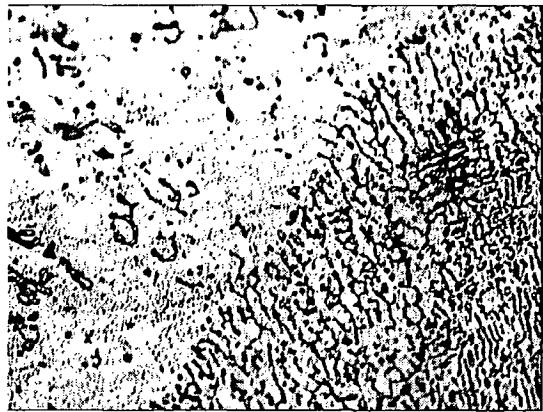
(e) HAZ, 100Hz (f) Fusion Boundary, 100 Hz

Figure 4.4: Optical micrograph of HAZ (a, c, e) and fusion boundary (b, d, f) of Alloy A weld joints produced using 25Hz, 50Hz and 100 Hz pulse frequency and 6ms pulse duration, 200 x.
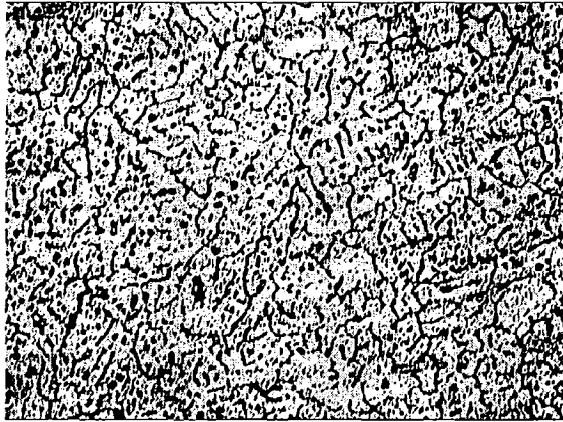
(a) 4ms and 25 HZ   (b) 6ms and 25 Hz
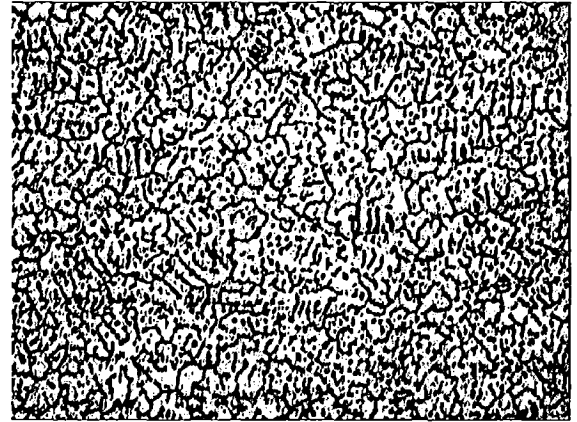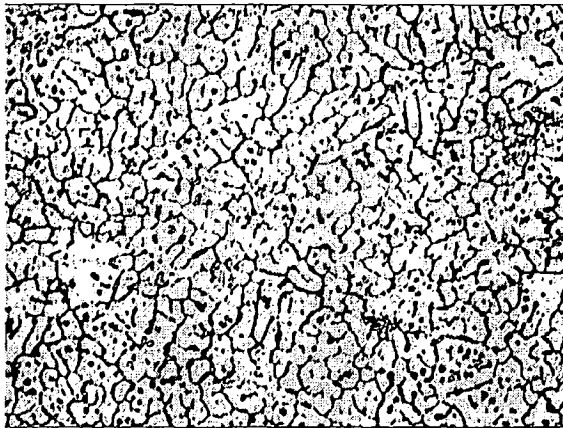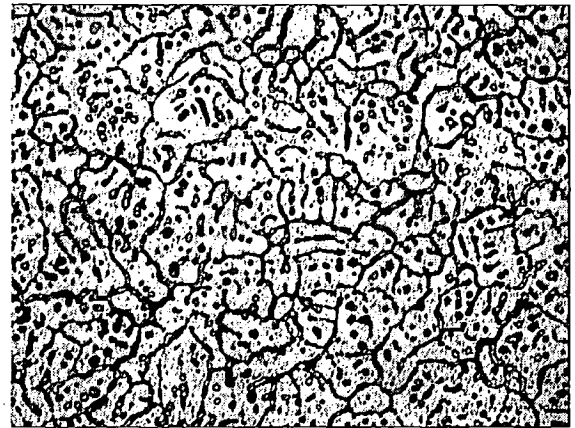
(c) 4ms and 50 Hz   (d) 6ms and 50 Hz
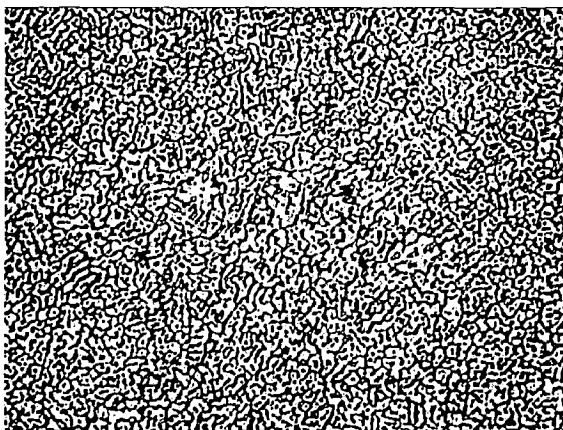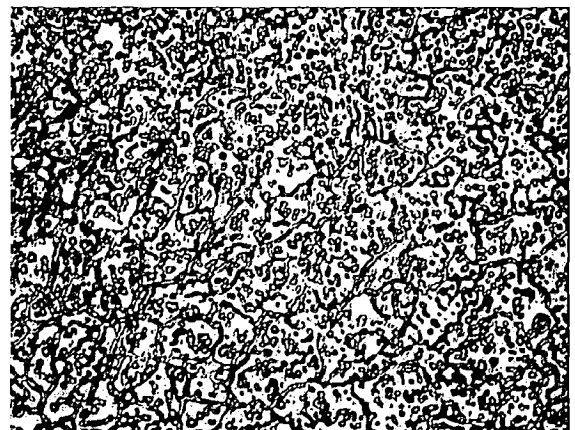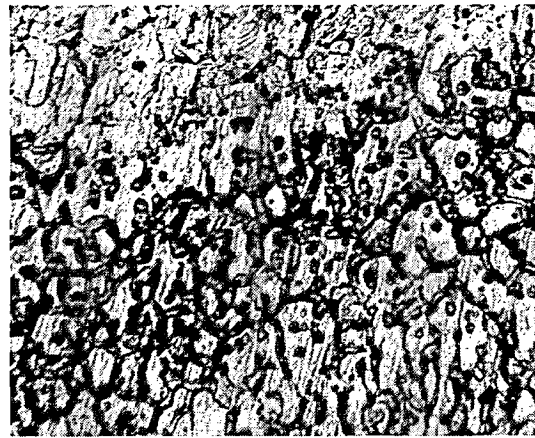
(e) 4ms and 100 Hz   (f) 6ms and 100 Hz

Figure 4.5: Optical micrograph showing the influence of pulse duration on microstructure of alloy B at different pulse frequencies (a) 4ms and 25 Hz (b) 6ms and 25 Hz(c) 4ms and 50 Hz (d) 6ms and 50 Hz (e) 4ms and 100 Hz (f) 6ms and 100 Hz, 200 ×.
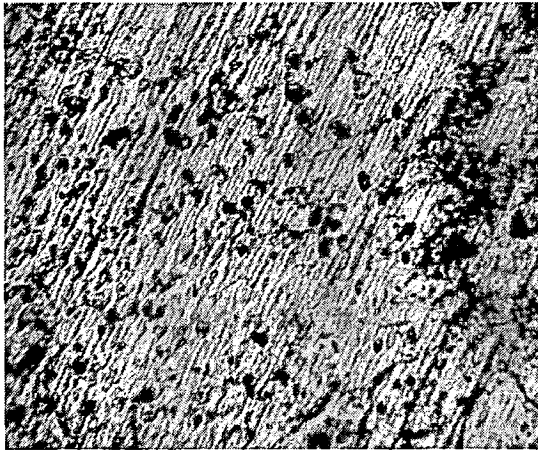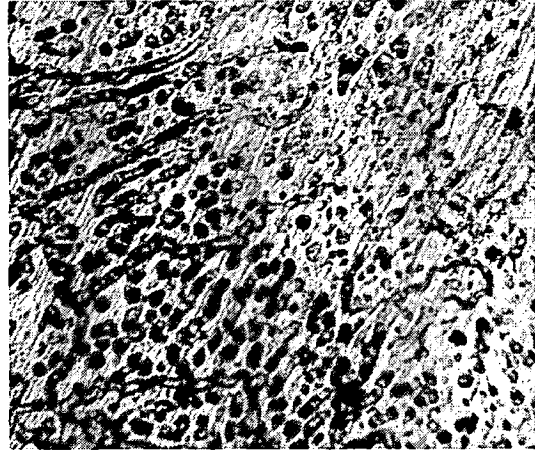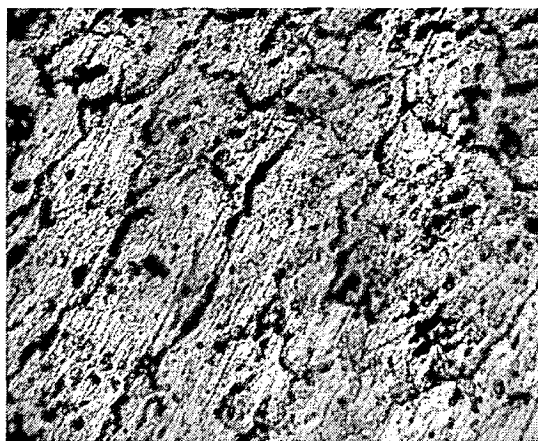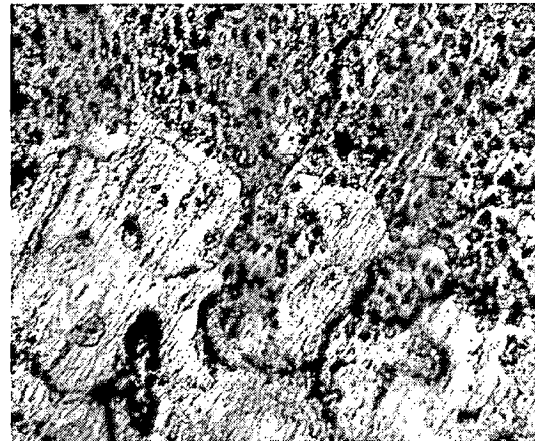
(a)HAZ, 25 Hz
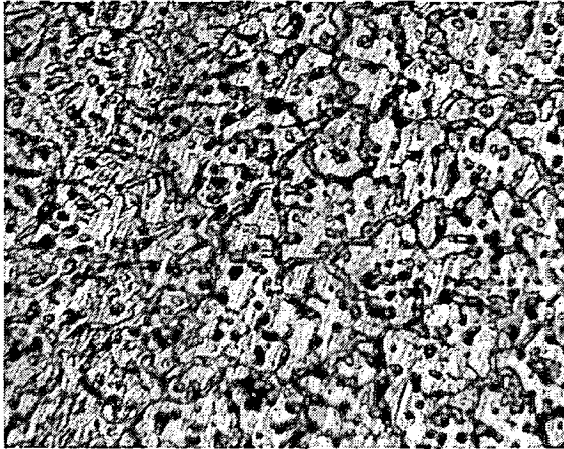(b)fusion, 25 Hz
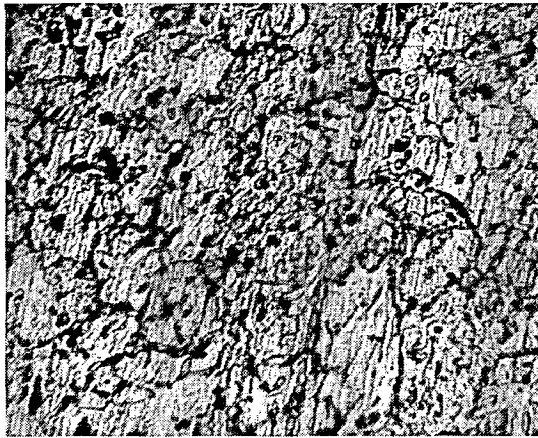
(c)HAZ, 33 Hz
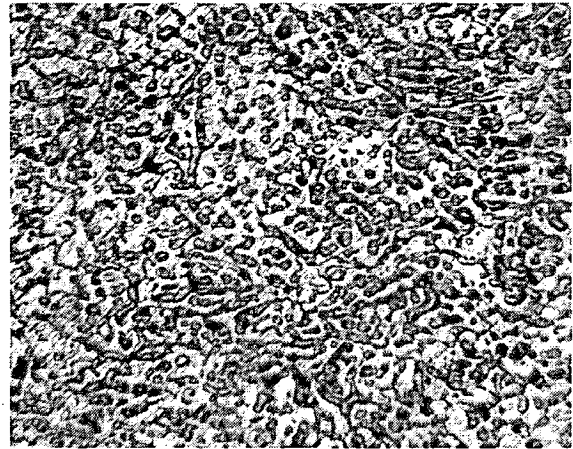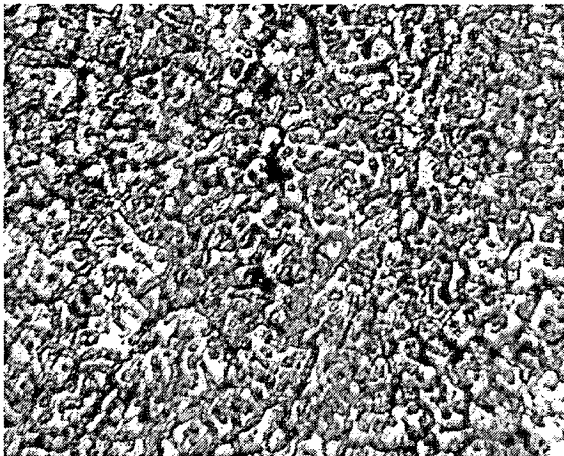(d)fusion, 33 Hz

(e) HAZ, 50 Hz
(f)fusion, 50 Hz

Figure 4.6. Optical micrograph of HAZ (a, c, e) and fusion boundary (b, d, f) of Alloy B weld joints produced using 25Hz, 33Hz and 50 Hz pulse frequency and 40% duty cycle, 200x.
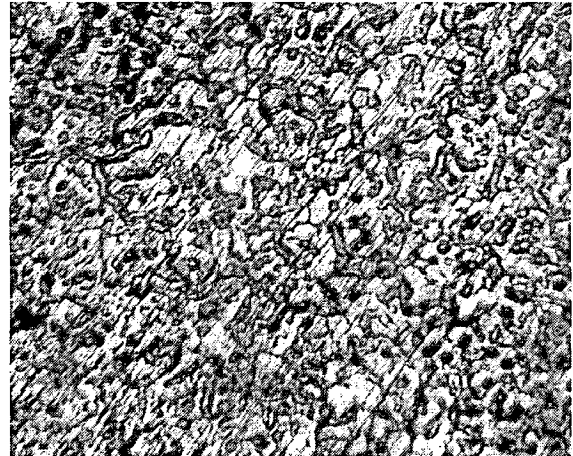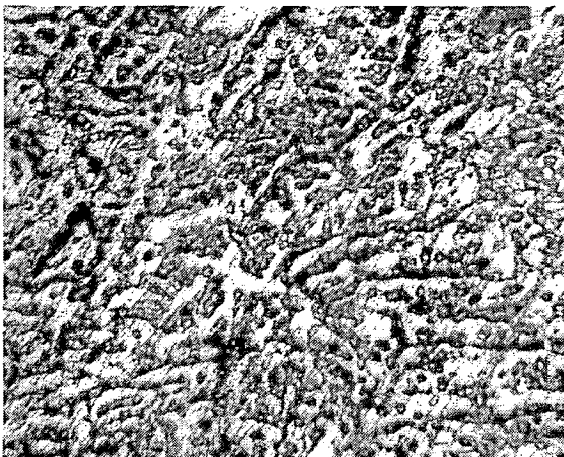
(a) 25Hz and 40% duty cycle
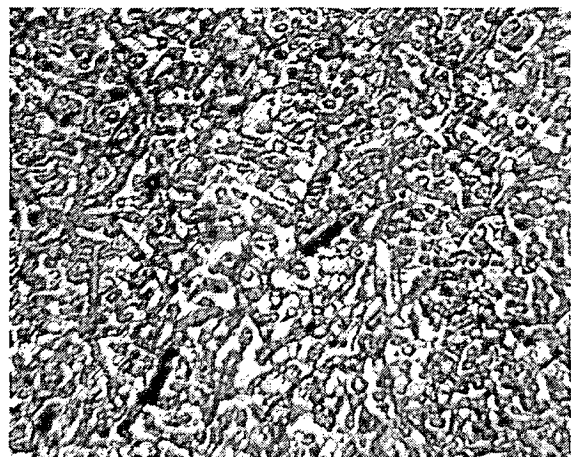
(b) 25Hz and 50% duty cycle

(c) 33Hz and 40% duty cycle

(d) 33Hz and 50% duty cycle

(e) 50Hz and 40% duty cycle

(f) 50Hz and 50% duty cycle

Figure 4.7: Optical micrograph showing the influence of duty cycle on microstructure of alloy B at different pulse frequencies (a) 40% and (b)50% duty cycles at 25 Hz (c) 40% and (d) 50% duty cycles at 33 Hz (e) 40% and (f) 50% duty cycles at 50 Hz, 200x.

Sl. No.	Specimen Designation	Mean Current (amp)	Pulse Duration (ms)	Pulse Frequency (Hz)	Micro hardness of alloy A (HV_{100})	Micro Hardness of alloy B (HV_{100})
1	100	160	--	0	72.63	67.43
2	142	160	4	25	63.05	68.97
3	145	160	4	50	64.65	70.29
4	141	160	4	100	84.58	81.54
5	162	160	6	25	64.76	65.13
6	165	160	6	50	71.51	73.91
7	161	160	6	100	64.16	62.74
8	200	180	--	0	72.48	71.16
9	242	180	4	25	69.49	69.59
10	245	180	4	50	70.83	67.5
11	241	180	4	100	87.50	71.89
12	262	180	6	25	67.47	67.7
13	265	180	6	50	69.31	71.9
14	261	180	6	100	67.24	62.65

Table 4.1: Influence of pulse parameters on Micro hardness of Alloy A and B(for first set of parameters).

Sl. No.	Back ground Current (amp)	Peak Current (amp)	Pulse Frequency (Hz)	Duty Cycle (%)	Specimen Designation	Micro Hardness of alloy A (HV_{100})	Micro Hardness of alloy B (HV_{100})
1	125	250	25	40	I	73.9	74.2
				50	II	72.4	75.0
2	125	250	33	40	III	66.0	78.0
				50	IV	69.4	72.7
3	125	250	50	40	V	64.2	74.2
				50	VI	75.7	78.8

Table 4.2.: Influence of pulse parameters on Microhardness of Alloys A and B(for second set of parameters).

Sl.No.	Specimen Designation	Mean Current (amp)	Pulse Duration (ms)	Pulse Frequency (Hz)	Macro hardness of alloy A (5 Kg)	Macro hardness of alloy B (5 Kg)
1	100	160	--	0	85	79.4
2	142	160	4	25	79.5	78.7
3	145	160	4	50	72.9	81.0
4	141	160	4	100	64.8	73.6
5	162	160	6	25	80.9	78.0
6	165	160	6	50	78.03	76.4
7	161	160	6	100	73.83	75.7
8	200	180	--	0	111.9	76.5
9	242	180	4	25	77.4	69.7
10	245	180	4	50	71.6	75.0
11	241	180	4	100	78.6	82.6
12	262	180	6	25	80.9	81.8
13	265	180	6	50	79.5	81.8
14	261	180	6	100	76.4	89.6

Table 4.3: Influence of pulse parameters on macro hardness of Alloy A and B (for first set of parameters).

Sl. No.	Back ground Current (amp)	Peak Current (amp)	Pulse Frequency (Hz)	Duty Cycle (%)	Specimen Designation	Macro Hardness of alloy A (5 Kg)	Macro Hardness of alloy B (5 Kg)
1	125	250	25	40	I	69.7	85.4
				50	II	75.9	81.0
2	125	250	33	40	III	72.9	79.8
				50	IV	74.4	77.9
3	125	250	50	40	V	73.0	70.5
				50	VI	69.6	73.0

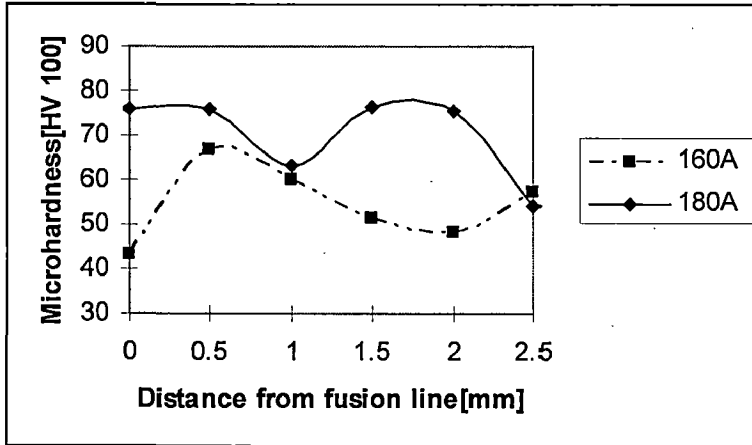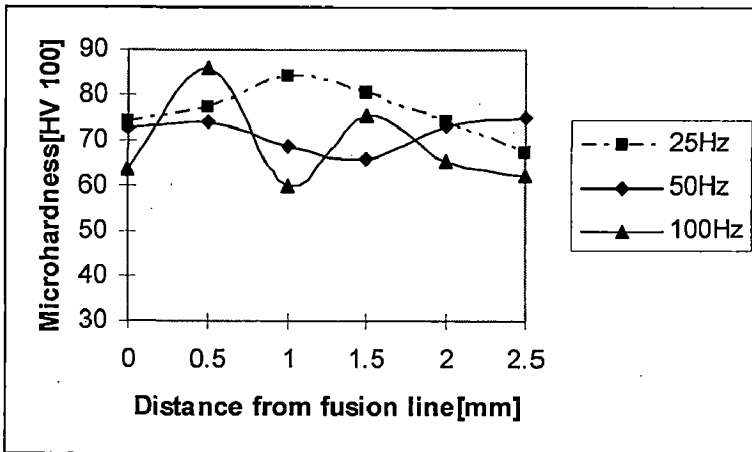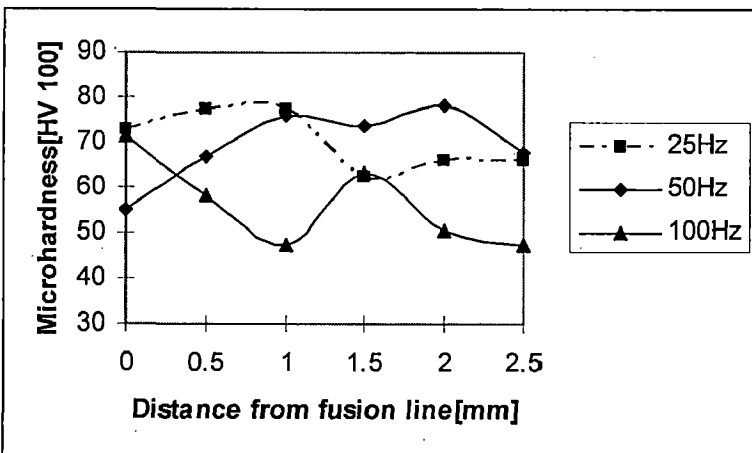Table 4.4: Influence of pulse parameters on macrohardness of Alloys A and B (for second set of parameters).

Fig.4.8. Micohardness vs. distance from fusion boundary relationship of HAZ of GTA weld joint of alloy A produced using two different welding currents.
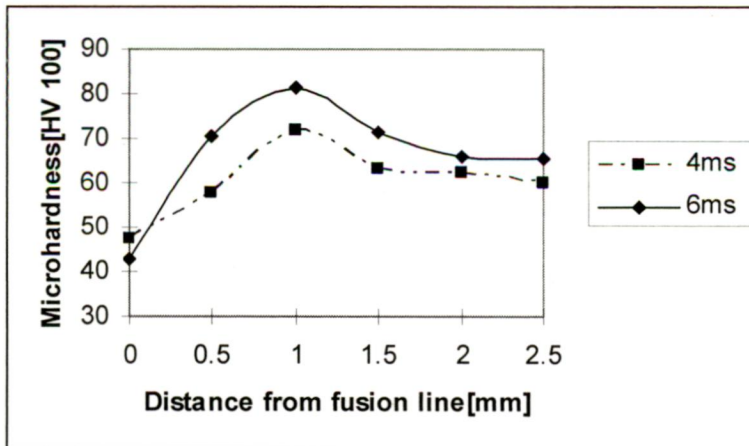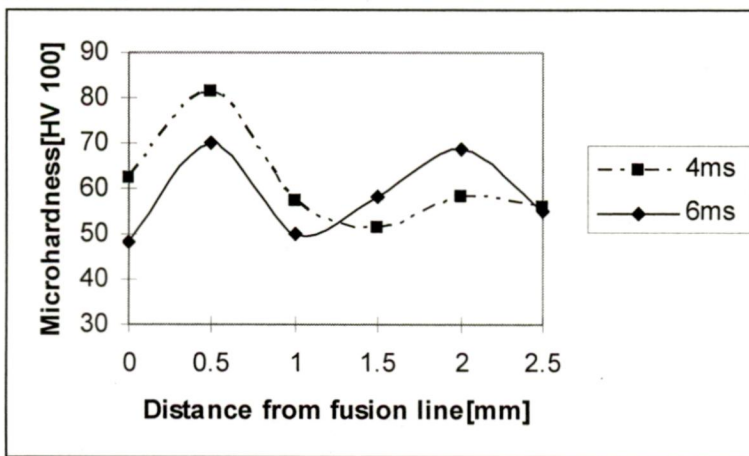

(a) 4ms pulse duration
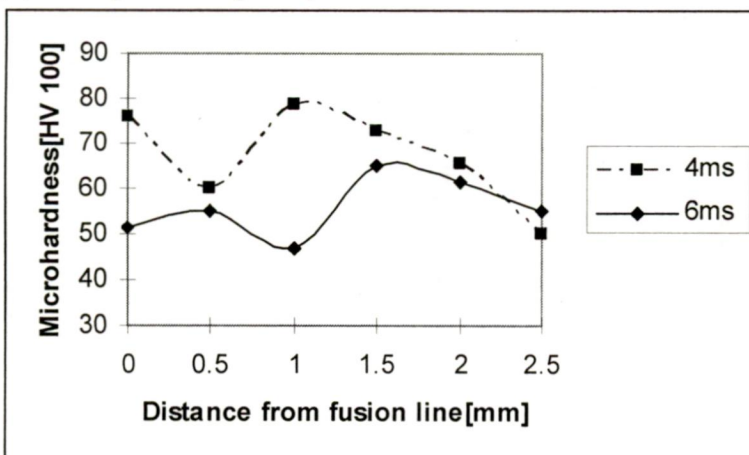

(b) 6ms pulse duration

Fig.4.9 Microhardness vs. distance from fusion boundary relationship of HAZ of weld joint of alloy B produced using three different pulse frequencies and two pulse duration (a) 4ms and (b) 6ms.

(a) 25Hz pulse frequency

(b) 50Hz pulse frequency
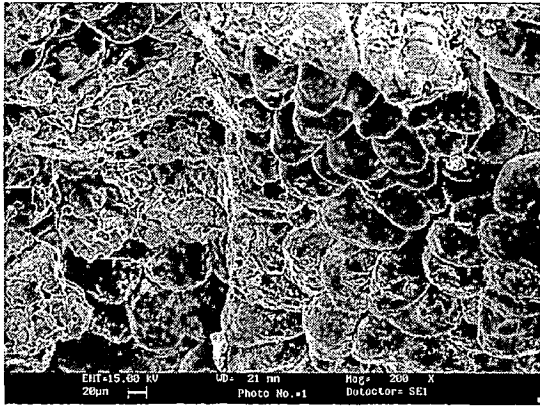

(c) 100Hz pulse frequency

Fig.4.10. microhardness vs. distance from fusion boundary relationship of HAZ of a weld joint of alloy A produced using two pulse duration and three pulse frequencies (a) 25Hz, (b) 50Hz, (c) 100Hz.

| Sl. No.	Back ground Current (amp)	Peak Current (amp)	Pulse Frequency (Hz)	Duty Cycle (%)	Specimen Designation	Ultimate Tensile Strength of alloy A (Mpa)	Ultimate Tensile Strength of alloy B (Mpa)
1	125	250	25	40	I	79.74	79.65
				50	II	67.09	76.39
2	125	250	33	40	III	62.25	62.73
				50	IV	60.64	62.89
3	125	250	50	40	V	55.22	71.53
				50	VI	57.59	78.48

Table 4.5: Influence of pulse parameters on Ultimate Tensile Strength of alloys A and B.

|	Microhardness of alloy A (100g)	Microhardness of alloy B (100g)	Macrohardness of alloy A (HV_{100})	Macrohardness of alloy B (HV_{100})
Without heat treatment	53.3	62.4	51.3	62.6
With heat heat treatment	71.3	72.7	75.9	80.2
With Solutionization	56.1	60.2	55.2	55.2
With artificial ageing	57.1	52.4	42.0	62.6

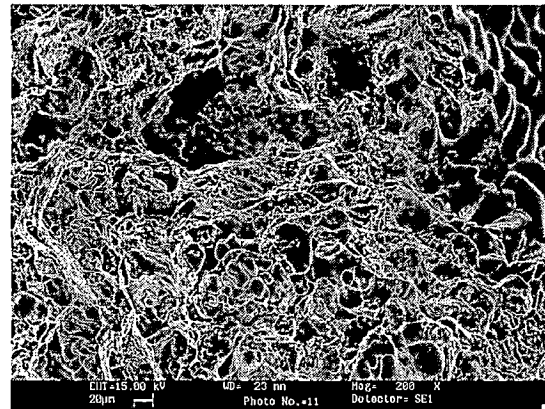Table 4.6: Influence of heat treatment on hardness of alloys A and B.

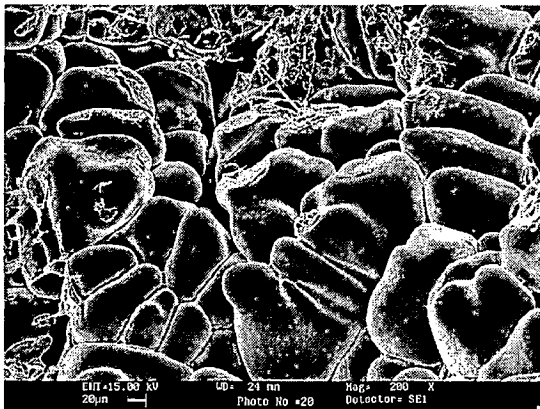(a) Alloy A, 25 Hz pulse frequency
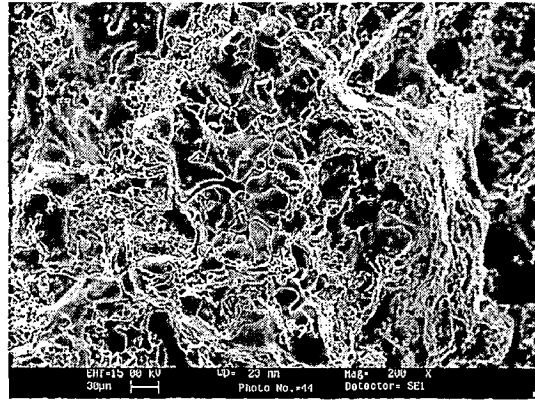
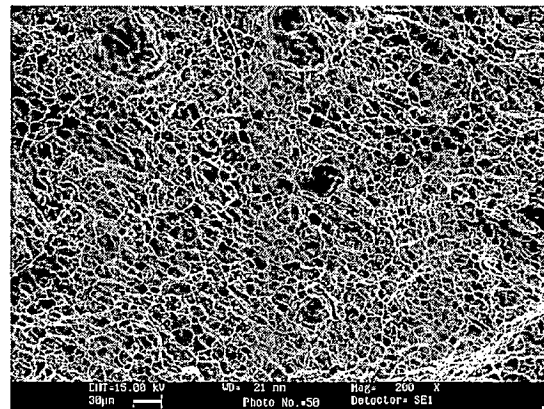(b) Alloy B, 25 Hz pulse frequency
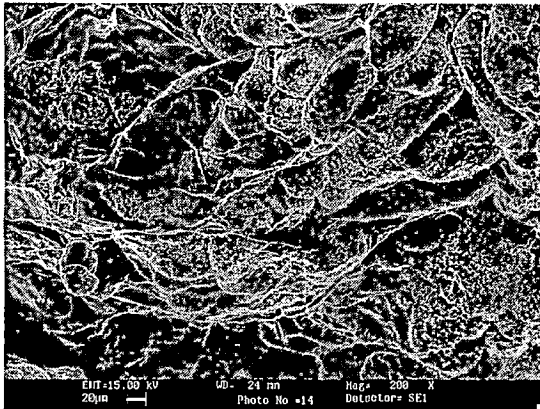
(c) Alloy A, 33 Hz pulse frequency
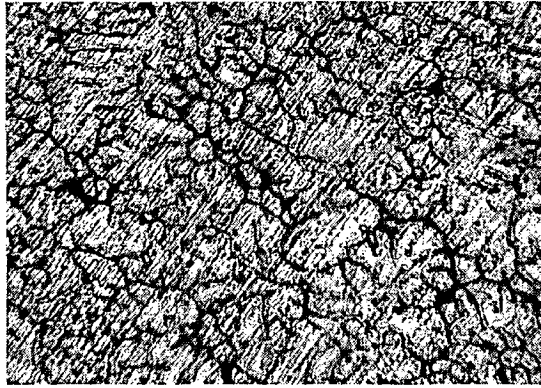

(d) Alloy B, 33 Hz pulse frequency

(e) Alloy A, 50 Hz pulse frequency
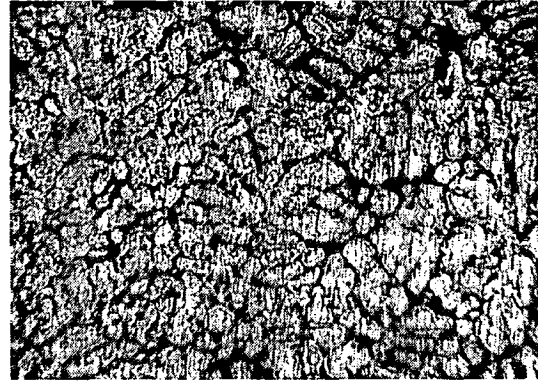

(f) Alloy B, 50 Hz pulse frequency

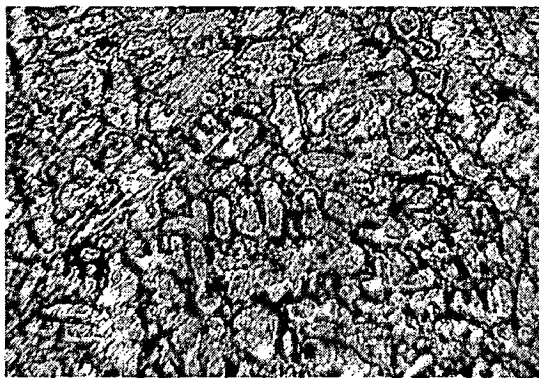Figure 4.11: SEM microphotographs of tensile fracture surfaces, 200 x.

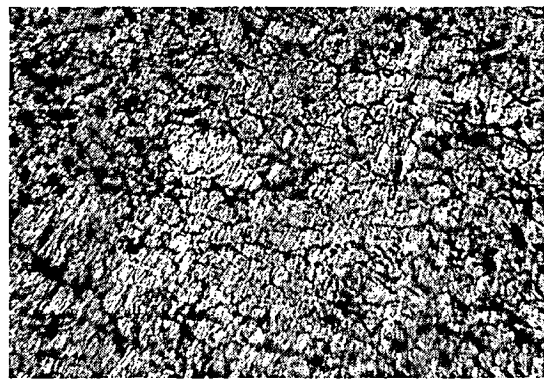(a) Alloy A   b)Alloy B

Figure 4.12 Optical micrograph showing the microstructure of alloys A and alloy B 200x.

(a)Alloy A, Heat Treated   (b) Alloy B , Heat Treated

Figure 4.13 Optical micrograph showing the influence solutionization and artificial ageing (T6 condition) on microstructure of (a) alloy A and (b) alloy B, 200x.

CONCLUSION

During Pulsed TIG welding of Al-Mg-Si alloy by using Al-5%Si filler wire, the pulse parameters such as peak current, pulse frequency, pulse duration and duty cycle are found to affect the microstructure and mechanical properties. Pulse TIG welding produced finer grain structure of weld metal than the conventional TIG welding (without pulsing).

Increase in pulse frequency refined the grain structure of weld metal when welding is done using short pulse duration. Influence of pulse frequency on grain structure appears to be governed by pulse duration. At same pulse frequency longer pulse duration produced the coarser structure than the short pulse duration. Increase in peak current also coarsens the grain structure.

Increased pulse frequency decreases the macrohardness of the weld metal when welding is done using lower peak current. An increase in microhardness was noticed with increase in pulse frequency. Hardness was found higher for shorter pulse duration.

Increase in pulse frequency reduced the tensile strength of weld metal irrespective of duty cycle. At same pulse frequency, lesser tensile strength was observed with longer duty cycles than shorter duty cycles.

REFERENCES

1. Parmar,R.S., Welding Processes and Technology:, Chapter 9, 227 to 249.Khanna Publishers, Delhi (1997).

2. Jean Cornu, Advanced Welding Systems , Vol. 3,IFS Publication Ltd.,U.K.(1988) 1 to 115.

3. John A.Francis, G.M.Delphine Cantin, The role of defects in the fracture of an Al-Si-Mg cast alloy , Materials Science and Engineering, A 407 (2005) 322-329.

4. Sargunam.M.S., A Study of Pulsed GTAW Process , Proceedings of International Welding Conference, New Delhi, India, Vol. 2,(1987) 799 to 803.

5. C.Huang and S.Kou, Liquation Cracking In Full-Penetration Al-Mg-Si Welds , Welding Journal,(April 2004) 112 to 116.

6. Metals handbook, 9th Ed., Vol.3,ASM International, Metals Park,Ohio, .97-98.

7. Welding Handbook, Fundamentals of Welding , Seventh Edition, Vol.1American Welding Society, Miami, .9 to 11.

8. Y.L.Liu and S.B.Kang, The solidification process of Al-Mg-Si alloys , Journal of Materials Science 32 (1997) 1443-1447.

9. G. Cao And S.Kou, Liquation Cracking In Full-Penetration Al-Si Welds , Welding Journal,(April 2005) .64 to 70.

10. C.H.Caceres and B.I Selling, Casting defects and the tensile properties of an Al-Si-Mg alloy , Materials Science and Engineering, A 220 (1996) 109-116.

11. Wang.Q.G. and Caceres.C.H., The fracture mode in Al-Mg-Si casting alloys , Materials Science and Engineering A241(1998)72-82.

12. D. Jiang and C. Wang, Influence of microstructure on deformation behavior and fracture mode of Al-Mg-Si alloys ,Materials Science and Engineering A, Volume 352, Issues 1-2,(15 July 2003) 29-33.